Degrees of lateralisation in semantic cognition: Evidence from intrinsic connectivity

Tirso Rene del Jesus Gonzalez Alam [a,b], Theodoros Karapanagiotidis [a,b], Jonathan Smallwood [a,b], Elizabeth Jefferies [a,b,*]

[a] Department of Psychology, University of York, YO10 5DD, UK
[b] York Neuroimaging Centre, Innovation Way, Heslington, York, YO10 5NY, UK

ABSTRACT

The semantic network is thought to include multiple components, including heteromodal conceptual representations and semantic control processes that shape retrieval to suit the circumstances. Much of this network is strongly left-lateralised; however, work to date has not considered whether separable components of semantic cognition have different degrees of lateralisation. This study examined intrinsic connectivity of four regions implicated in heteromodal semantic cognition, identified using large scale meta-analyses: two sites which have been argued to act as heteromodal semantic hubs in anterior temporal lobe (ATL) and angular gyrus (AG); and two sites implicated in semantic control in inferior frontal (IFG) and posterior middle temporal gyri (pMTG). We compared the intrinsic connectivity of these sites in left hemisphere (LH) and right hemisphere (RH), and linked individual differences in the strength of within- and between-hemisphere connectivity from left-lateralised seeds to performance on semantic tasks, in a sample of 196 healthy volunteers. ATL showed more symmetrical patterns of intrinsic connectivity than the other three sites. The connectivity between IFG and pMTG was stronger in the LH than the RH, suggesting that the semantic control network is strongly left-lateralised. The degree of hemispheric lateralisation also predicted behaviour: participants with stronger intrinsic connectivity *within* the LH had better semantic performance, while those with stronger intrinsic connectivity *between* left pMTG and homotopes of semantic regions in the RH performed more poorly on judgements of weak associations, which require greater control. Stronger connectivity between left AG and visual cortex was also linked to poorer perceptual performance. Overall, our results show that hemispheric lateralisation is particularly important for the semantic control network, and that this lateralisation has contrasting functional consequences for the retrieval of dominant and subordinate aspects of knowledge.

1. Introduction

Semantic cognition allows us to understand the meanings of words, images, sounds, actions and events, and to flexibly use our knowledge to drive thoughts and behaviours that are appropriate to our goals and the current context (Jefferies, 2013; Lambon Ralph et al., 2017). Since we know many features and associations for any given concept, semantic cognition is thought to reflect the interaction of at least two separable neurocognitive components: (i) long-term heteromodal semantic representations and (ii) control processes that focus retrieval on aspects of knowledge that are currently relevant, even when these are non-dominant (Chiou et al., 2018; Hoffman et al., 2018; Jefferies, 2013;

Lambon Ralph et al., 2017; Noonan et al., 2013). Contemporary accounts of semantic cognition, such as the Controlled Semantic Cognition framework, propose that these interacting elements are supported by dissociable cortical regions within the semantic network, which is largely left-lateralised (Lambon Ralph et al., 2017; Davey et al., 2016). However, the degree of lateralisation might vary across the neurocognitive components that support semantic representation and control.

Heteromodal concepts are thought to be represented bilaterally, in ventral aspects of the anterior temporal lobes (ATL; Hub and Spoke model, Lambon Ralph et al., 2017; Patterson et al., 2007; Rogers et al., 2006). This site is thought to act as a "hub" allowing the integration of diverse features, including visual, auditory, motor, linguistic, praxis and

valence information (stored within "spokes"). Semantic dementia, which is associated with marked degradation of conceptual knowledge across modalities, follows bilateral atrophy of ventral ATL; cases with unilateral ATL lesions have less pronounced semantic deficits (Lambon Ralph et al., 2010; Rice et al., 2018a), suggesting that conceptual knowledge is distributed across both hemispheres. Nevertheless, even within a bilateral system, there can be some degree of lateralisation. Patients with more left than right-sided ATL damage often show greater difficulties with verbal semantic access, while those with the converse pattern can show greater impairment on pictorial and social semantic tasks (Lambon Ralph et al., 2001; Mion et al., 2010; Rice et al., 2018a; Snowden et al., 2004; Thompson et al., 2003). Similarly, while neuroimaging meta-analyses show bilateral ATL activation across word and picture semantic tasks (see Fig. 3), this response is more strongly left-lateralised for tasks involving written words and language production (Rice et al., 2015b).

In contrast to the bilateral response in ATL, other sites in the semantic network typically show little or no response in the RH. Left but not right AG is implicated in semantic cognition (Binder et al., 2009)– with a recent meta-analysis linking AG with 'automatic' aspects of semantic retrieval (Davey et al., 2015; Humphreys and Lambon Ralph, 2015), although its contribution to semantic cognition remains unclear (Humphreys et al., 2015). ATL and AG are commonly implicated in processing coherent conceptual combinations (Bemis and Pylkkänen, 2013; Davey et al., 2015; Price et al., 2015; Teige et al., 2018) and both are argued to act as heteromodal 'hub' regions (Reilly et al., 2016; Seghier, 2012). AG also shows relatively strong intrinsic connectivity to lateral parts of ATL (Bellana et al., 2016; Davey et al., 2016, 2015; Hurley et al., 2015; Jackson et al., 2017) and both sites show a pattern of intrinsic connectivity allied to the default mode network (DMN) – at least when contrasted with semantic regions that support control processes. However, there are functional subdivisions in both regions: the ventral ATL site, thought to act as a heteromodal hub, is *not* a core region within DMN (Jackson et al., 2019).

Other left-lateralised parts of the semantic network – namely left IFG and pMTG – are thought to support semantic control processes (Badre et al., 2005; Hallam et al., 2016; Noonan et al., 2013; Thompson-Schill et al., 1997; X. Wang et al., 2018). Neuroimaging studies show consistent activation of left IFG and pMTG in control-demanding semantic tasks involving weak associations, ambiguous words or strong distractors (Noonan et al., 2013), across both verbal and non-verbal tasks (Krieger-Redwood et al., 2015). Damage or inhibitory stimulation to either left IFG or pMTG elicits difficulty in semantic tasks with high but not low control demands (Davey et al., 2015; Jefferies and Lambon Ralph, 2006; Whitney et al., 2011), while disruption of left IFG elicits compensatory increases in pMTG recruitment (Hallam et al., 2018, 2016). Right IFG also shows some activation in contrasts tapping semantic control, although this response is weaker and less extensive than in left IFG (Noonan et al., 2013), and activation in right pMTG is rarely observed. Interestingly, although sites activated in semantic control partially overlap with bilateral multiple-demand network (MDN) regions (Davey et al., 2016; Noonan et al., 2013), the peak semantic response in left IFG and pMTG is outside the executive network (Gonzalez Alam et al., 2018). We recently suggested that LH semantic control regions sit at the juxtaposition of DMN and multiple-demand cortex, suggesting they might help to integrate processes supported by these networks, which are normally anti-correlated (Davey et al., 2016). Yet these large-scale networks (DMN and MDN) are bilateral and largely symmetrical, raising the question of why semantic cognition is left-lateralised.

This study examined connectivity differences for LH semantic regions and their homotopes in the RH, to see if this can explain semantic lateralisation. Previous work has already shown stronger intrinsic connectivity in left than right ATL to other LH semantic sites (Hurley et al., 2015). Left IFG and pMTG have strong intrinsic connectivity, consistent with the view they form a left-lateralised network for semantic control (Davey et al., 2016; Hallam et al., 2018; Hurley et al., 2015; X. Wang

et al., 2018), although the comparison with RH connectivity has been little explored. Left AG also shows stronger connectivity than right AG to semantically-relevant lateral temporal regions during memory retrieval (Bellana et al., 2016). This study extends this research to characterise hemispheric differences across four key semantic sites, within the same participants, allowing us to compare the degree of lateralisation for semantic representation and control sites for the first time.

We first examine the connectivity profiles of four key sites – ventral ATL, AG, pMTG and IFG – which are implicated in heteromodal semantic cognition by neuroimaging meta-analyses. We characterise the intrinsic connectivity of these LH sites and their RH homotopes in 196 participants who completed a resting-state scan, and quantify (i) simple differences in connectivity across hemispheres (by computing contrasts between LH and RH seeds, which are largely symmetrical); and (ii) regions in which left-lateralised and right-lateralised patterns of connectivity show topographic differences. We also examine overlap in the connectivity patterns of these semantic sites within each hemisphere to establish whether regions thought to support semantic control (i.e. IFG and pMTG) show stronger connectivity to each other than other semantic sites (ATL and AG), and whether this pattern varies across the hemispheres. We use meta-analytic decoding to examine the likely functional consequences of asymmetries in connectivity.

Next, we investigate how individual differences in the intrinsic connectivity of the four left-lateralised semantic sites is related to individual variation in the efficiency of semantic retrieval, relative to perceptual judgements. In order to test the multiple component account of semantic cognition, in which different patterns of connectivity might be critical for heteromodal conceptual representation and control, we contrast different semantic tasks, involving the comprehension of words and pictures, as well as the retrieval of strong and weak associations that differ in their semantic control demands. We test the hypothesis that within-hemisphere connectivity from left-sided seeds may be associated with good semantic performance, while controlled semantic retrieval may be weaker in participants who have more cross-hemisphere connectivity, since the semantic control network is thought to be strongly left-lateralised. To anticipate, we also observe distinct patterns of connectivity, which are associated with semantic and language processing in LH, and visual perception and spatial processing in the RH. We find that ATL has more symmetrical intrinsic connectivity than the other sites. In contrast, the semantic control network is more strongly left-lateralised, and this pattern of lateralisation is associated with efficient semantic retrieval.

2. Methods

2.1. Overview

This study was approved by the local research ethics committees. The data were obtained as part of a large cohort study, consisting of resting state fMRI and a battery of cognitive assessments in 207 healthy young adult volunteers (137 females; age: mean $\pm$ SD $= 20.21 \pm 2.35$, range: 18–31 years). Elements of this cohort study have been described previously in papers focussing on mind-wandering (Poerio et al., 2017; Sormaz et al., 2018; Turnbull et al., 2018; H. T. Wang et al., 2018a, 2018b), the functional consequences of hippocampal connectivity (Karapanagiotidis et al., 2017; Sormaz et al., 2017), patterns of semantic performance linked to individual differences in connectivity within LH semantic sites falling in different networks (Vatansever et al., 2017) and cortical thickness (X. Wang et al., 2018). No previous studies using this cohort have examined semantic performance in relation to hemispheric differences.

The analysis was divided into three steps. (i) We compared the intrinsic connectivity of four heteromodal semantic ROIs in the LH (ATL, AG, IFG, pMTG) with RH homotopes. The ROIs were identified using activation likelihood estimation meta-analytic maps of semantic processing (Humphreys and Lambon Ralph, 2015; Noonan et al., 2013; Rice

et al., 2018b). We compared patterns of connectivity across pairs of seeds implicated in semantic control (pMTG and IFG) and not implicated in semantic control (ATL and AG). (ii) We also quantified the extent to which LH seeds and their RH homotopes showed symmetrical patterns of connectivity. We performed meta-analytic decoding using Neurosynth (Gorgolewski et al., 2015; Yarkoni et al., 2011) to identify psychological terms associated with LH vs. RH connectivity from these individual seeds. (iii) We then assessed whether individual differences in the intrinsic functional connectivity of the LH seeds would predict variation in performance on semantic and non-semantic tasks. Our semantic battery allowed a comparison not only of semantic and non-semantic decisions, but also of different types of semantic judgement (strong and weak thematic associations, which differ in their requirement for controlled semantic retrieval, and word vs. picture-based judgements). If semantic control is strongly left-lateralised, we might expect within-hemisphere connectivity to show an association with better performance, while cross-hemisphere connectivity from LH seeds to semantic homotopes in the RH might relate to poorer control over retrieval. We elected to focus on LH seeds since all four LH seeds are implicated in semantic processing, while this is not the case for all the RH seeds. This decision also allowed us to avoid the inflation of type I error which would arise from examining many seeds. Since bilateral ATL is implicated in semantic processing, we also examined behavioural associations with right ATL connectivity in a supplementary analysis, but found no significant effects.

2.2. Participants

The analysis was based on 196 participants out of 207 (126 females; mean $\pm$ SD age $= 20.1 \pm 2.3$ years), recruited from the undergraduate and postgraduate student body at the University of York. The participants were right handed, native English speakers with normal/corrected vision. None of them had a history of psychiatric or neurological illness, severe claustrophobia, drug use that could alter cognitive functioning, or pregnancy. We excluded eleven participants: two due to missing MRI data and nine due to missing behavioural data. All volunteers provided written informed consent and were either paid or given course credit for their participation.

2.3. Procedure

The participants first took part in a neuroimaging session, where we acquired structural images and a resting-state scan. Participants then completed numerous cognitive assessments across three sessions, each lasting around 2 h, with the order of the sessions counterbalanced across participants. This study provides an analysis of the semantic battery administered as part of this protocol.

2.4. Tasks

We manipulated decision type (semantic/non-semantic), modality (words/pictures) and strength of association (weak/strong associates). All tasks employed a three-alternative forced-choice design: participants matched a probe stimulus on the screen with one of three possible targets, and pressed buttons to indicate their choice.

We compared semantic relatedness judgements to words and pictures to verify whether patterns of connectivity from heteromodal LH seeds predicted performance across modalities (Rice et al., 2015b). We also manipulated strength of association in a picture-word matching task. Strength of association is thought to modulate the 'controlled retrieval' demands of semantic judgements; weak associations elicit stronger activation in the semantic control network, in both left pMTG and IFG (Badre et al., 2005; Davey et al., 2016; Noppeney et al., 2004; Wagner et al., 2001). In contrast, semantic control demands are minimised during the retrieval of strong associations, since the target is a dominant associate of the probe. Consequently, individual differences in intrinsic connectivity from LH semantic control seeds might relate to performance

differences between weak and strong associations. Finally, we included a non-semantic task involving perceptual judgements. Participants were asked to select which scrambled picture was an exact match to a probe image.

In all tasks, each trial consisted of a centrally-presented probe presented with a target and two unrelated distractors, which were targets in other trials. Each trial started with a blank screen for 500 m s. The response options were subsequently presented at the bottom of the screen for 900 m s (with the three options aligned horizontally, and the target in each location equally often). Finally, the probe was presented at the top of the screen. The probe and choices remained visible until the participant responded, or for a maximum of 3 s. Both response time (RT) and accuracy were recorded, and an efficiency score was calculated for each participant in each condition by dividing response times by accuracy (note: in brain analyses, this efficiency score was inverted to aid the interpretation of the results, such that a higher score corresponded to better performance). Fig. 1 illustrates the tasks and summarises the behavioural results.

The stimuli employed in the tasks were selected from a larger dataset of words and photographs used in previous experiments (Davey et al., 2015; Krieger-Redwood et al., 2015). The pictures were coloured photographs collected from the internet and re-sized to fit the trial structure (200 pixels, 72 dpi). All the coloured pictures and words were rated for familiarity using 7-point Likert scales, and imageability (>500) from the MRC psycholinguistic database (Coltheart, 1981; Wilson, 1988). Lexical frequency for the words was obtained by the SUBTLEX-UK database (van Heuven et al., 2014) to allow matching on psycholinguistic properties. Specific details for each task are provided below.

2.4.1. Word-picture matching manipulating strength of association

Participants were asked to select the target word that was most strongly associated with a probe picture. The probe list included 60 coloured pictures (e.g., dog) which were paired with 60 strongly related (e.g., bone) and 60 weakly related targets (e.g., ball), presented as written words. The strength of association between probe-target pairs was assessed using a 7-point Likert scale and differed significantly between conditions (Table 1). There were no differences between strong and weak associations in word length, familiarity, imageability or lexical frequency (Table 1). These 120 trials were presented in four blocks of thirty trials each, and both strong and weak associations were presented in each block. The order of trials within the blocks was randomized across subjects. The presentation of the blocks was interleaved with blocks of the other semantic and non-semantic judgements.

2.4.2. Input modality: picture-picture vs. word-word association matching

Additional judgements of semantic association were presented using only written words, or coloured pictures (60 trials for each). In these trials, the probe and the response options were all presented in the same modality (i.e., word probes were presented with word responses). The two sets of target concepts did not differ in terms of mean word length, familiarity, imageability, lexical frequency and strength of association (Table 1). The task was split in four blocks of 30 trials each. The order of trials within the blocks was randomized across subjects. The presentation of the blocks was interleaved with the blocks of the other tasks.

2.4.3. Non-semantic perceptual matching task

This perceptual control task had decision-making demands that were similar to the semantic judgments (cf. Visser et al., 2012). The stimuli were 60 pixelated and scrambled black-and-white photographs of faces. Participants were asked to select the target that was identical to the probe; the distractors were the same images rotated by 180° or 270° (see Fig. 1 for an example). The task was split in two blocks of 30 trials each. The presentation of the blocks was interleaved with the blocks of the other tasks.
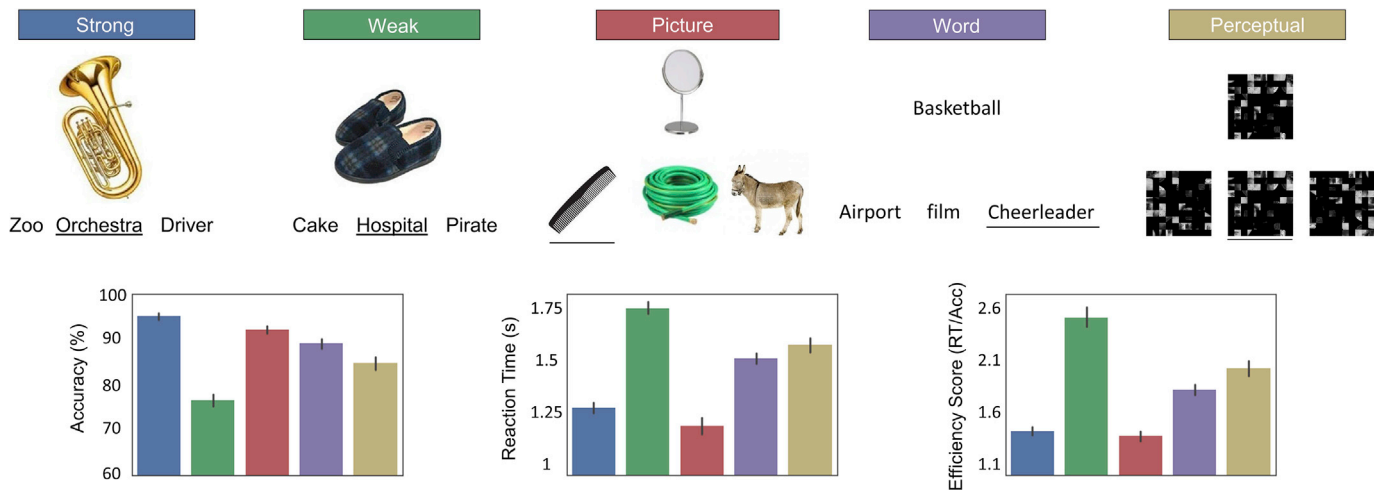
Fig. 1. Top row: Illustration of the behavioural tasks. For all the tasks, correct answers are underlined. The weak and strong associations involved Picture-Word matching. The layout of the Word-Word and Picture-Picture conditions was identical, except all the stimuli were either words or pictures. The perceptual matching task required participants to identify a complex item that was visually identical to the probe. Bottom row: Plots depicting the mean accuracy, reaction time and efficiency score (not reversed) for each task. The colour of each bar corresponds to the names of the tasks in the top row. Error bars represent 95% confidence intervals. All conditions were significantly different to each other in average efficiency score ($p < .001$, see Results section below).

Table 1
Psycholinguistic variables for our semantic battery by strength of association and modality.

	Strength of association				Modality			
	Strong	Weak	t	Sig.	Word	Picture	t	Sig.
	Mean (Standard errors)				Mean (Standard errors)			
Word Length	6.43 (.39)	6.6 (.34)	-.16	.873	6.08 (.31)	6.4 (.32)	-.69	.490
Lexical Frequency	13564.8 (1887)	11233.6 (1805)	.89	.374	4619.8 (823.1)	6458.7 (827.5)	-1.56	.122
Familiarity	6.02 (.09)	6.12 (.08)	-.88	.381	6.04 (.1)	5.98 (.1)	.40	.688
Imageability	5.16 (.13)	4.96 (.13)	1.07	.287	4.96 (.13)	4.97 (.12)	-.07	.948
Semantic Association	6.02 (.07)	3.32 (.10)	21.74	.000	4.80 (.14)	4.95 (.15)	-.76	.447

2.5. Neuroimaging

2.5.1. MRI data acquisition

MRI data was acquired using a 3T GE HDx Excite Magnetic Resonance Imaging (MRI) system utilising an eight-channel phased array head coil tuned to 127.4 MHz, at the York Neuroimaging Centre, University of York. Structural MRI acquisition in all participants was based on a T1-weighted 3D fast spoiled gradient echo sequence (TR = 7.8 s, TE = minimum full, flip angle = 20°, matrix size = 256 × 256, 176 slices, voxel size = 1.13 × 1.13 × 1 mm). A nine-minute resting state fMRI scan was carried out using single-shot 2D gradient-echo-planar imaging (TR = 3s, TE = minimum full, flip angle = 90°, matrix size = 64 × 64, 60 slices, voxel size = 3 × 3 × 3 mm^3, 180 vol). Participants were asked to passively view a fixation cross and not to think of anything in particular during the resting-state scan. A FLAIR scan with the same orientation as the functional scans was collected to improve co-registration between subject-specific structural and functional scans.

2.5.2. Pre-processing

All pre-processing of resting-state data used FMRIB Software Library (FSL version 4.1, http://fsl.fmrib.ox.ac.uk/fsl/). The Brain Extraction Tool (BET) was used to extract individual FLAIR and T1 weighted structural brain images (Smith, 2002). Structural images were linearly co-registered to the MNI 152 standard template using FMRIB's Linear Image Registration Tool (FLIRT, Jenkinson et al., 2002; Jenkinson and Smith, 2001). FMRI Expert Analysis Tool (FEAT Version 5.98, part of FSL) was used to perform the following standard analysis steps: (1) correcting for head movement using MCFLIRT (Jenkinson et al., 2002); (2) slice timing correction using Fourier space time-series phase-shifting;

(3) spatial smoothing with a 6 mm full-width half-maximum (FWHM) Gaussian kernel; (4) grand mean intensity normalisation of the entire 4D dataset by a single multiplicative factor; (5) high pass (sigma = 100s) and low pass (sigma = 2.8s) temporal filtering (Gaussian-weighted least-squares straight line fitting).

2.5.3. ROI selection

Fig. 3 (top row) shows an automated meta-analysis for the term "semantic". There is a strongly left-lateralised response to semantic tasks in four key regions: ATL, AG, IFG and pMTG, which we investigated in this study. Semantic cognition also elicits a response in dorsal anterior cingulate; however, since our focus was on hemispheric asymmetry, we excluded this medial region.

We identified co-ordinates for our ROIs from three neuroimaging meta-analyses of semantic cognition. (i) We selected an ATL seed from an average of peaks across eight studies that included a semantic > non-semantic contrast (Rice et al., 2018b), providing a peak response in left ventral ATL (MNI coordinates −41, −15, −31). (ii) Left AG also commonly shows activation during semantic tasks, when contrasted with non-semantic decisions that are at least as difficult (Binder et al., 2009). Our AG seed was taken from an ALE meta-analysis of 386 studies (Humphreys and Lambon Ralph, 2015), which identified a peak for automatic semantic retrieval in left AG (MNI -48, −68, 28). (iii) To identify ROIs associated with semantic control, we used an ALE meta-analysis of 53 studies (Noonan et al., 2013), which manipulated the control demands of semantic judgements in diverse ways (strength of association, ambiguous words, strength of distractors). This identified activation peaks in left IFG (MNI -47, 21, 18) and pMTG (MNI -58, −49, −9). To create ROIs, we placed a binarised spherical mask with a radius

of 3 mm, centred on the MNI coordinates of the peak response in each site. We generated right-hemisphere homotopic spheres for each seed by following the same procedure, but flipping the sign of the x coordinate in MNI space from negative to positive. An advantage of this sign-flipping method is that it allowed us to generate symmetrical seeds for all sites in a comparable way, even for sites that typically do not show a semantic response in the RH (e.g. for pMTG). However, there is good evidence of bilateral engagement of ATL in semantic cognition. Moreover, Rice et al. (2018b) identified a right ATL peak (MNI 44, -11, −36), which was not in an identical location to that in the LH. We replicated all of our analysis in the pipeline using this RH seed, instead of the sign-flipped homotope, in Supplementary Analysis S1. The results across the two ATL seeds were similar.

2.5.4. Analysis of intrinsic connectivity of ROIs

In a first-level analysis, we extracted the time series from each ROI. These were used as Explanatory Variables (EVs) in separate connectivity analyses for each seed (eight seeds in total: four LH seeds and their RH homotopes). In each analysis, eleven nuisance regressors were removed, including the confounding six head motion parameters and the top five principal components extracted from white matter (WM) and cerebrospinal fluid (CSF) masks using the CompCor method (Behzadi et al., 2007). These masks were generated from each individual's structural image (Zhang et al., 2001). We did not perform global signal regression which has been reported to introduce spurious anti-correlations (Murphy et al., 2009).

At the group level, analyses were carried out using FMRIB's Local Analysis of Mixed Effects (FLAME1) with automatic outlier detection (Beckmann et al., 2003; Woolrich, 2008; Woolrich et al., 2004). Significant clusters ($p < .05$) were defined using Gaussian random field theory with a voxel inclusion threshold of $z = 3.1$ to define contiguous clusters (Eklund et al., 2016).

2.5.5. Characterising hemispheric similarities and differences in intrinsic connectivity

Having characterised the whole-brain intrinsic connectivity of each site, we directly compared connectivity across the hemispheres. We took the intrinsic connectivity of single seeds at the individual level and defined a second level analysis including the LH and RH seeds as two EVs, including two contrasts: left > right seed connectivity and the reverse. Significant clusters at the group level were defined as above.

This direct comparison of LH and RH seeds yielded largely left-lateralised regions for the left > right connectivity contrast and largely right-lateralised regions for the reverse contrast. These two lateralised maps had similar shapes, although there were some asymmetries. In order to identify regions in which these patterns of differential connectivity varied across the hemispheres, we performed a second difference analysis. We projected the RH connectivity map into LH coordinate space for each participant (using the tool 'fslswapdim' in FSL 4.1. specifying as the only transformation the inversion of the x axis). This allowed us to perform a direct comparison of the shapes of the connectivity patterns for LH and RH. This is akin to the 'Flip Method' described in Baciu et al. (2005). At the group level, we again defined two contrasts: left > right flipped hemisphere connectivity and the reverse. The flip method therefore identified regions where LH seeds showed heightened connectivity, compared to the expected pattern from RH. Fig. 2 provides a summary of the analysis pipeline.

We examined the conjunctions for pairs of seed regions allied to (i) the semantic control network (IFG and pMTG) and (ii) not implicated in semantic control (ATL and AG), to identify voxels connected to both regions using the 'easythresh_conj' tool in FSL ($Z = 3.1$, $p = .05$); we did this for the LH and RH group maps resulting from 2.5.4 separately. We then computed voxels that were common for each conjunction in both hemispheres performing a binarised multiplication of the LH and the RH conjunction maps for each conjunction separately. Supplementary
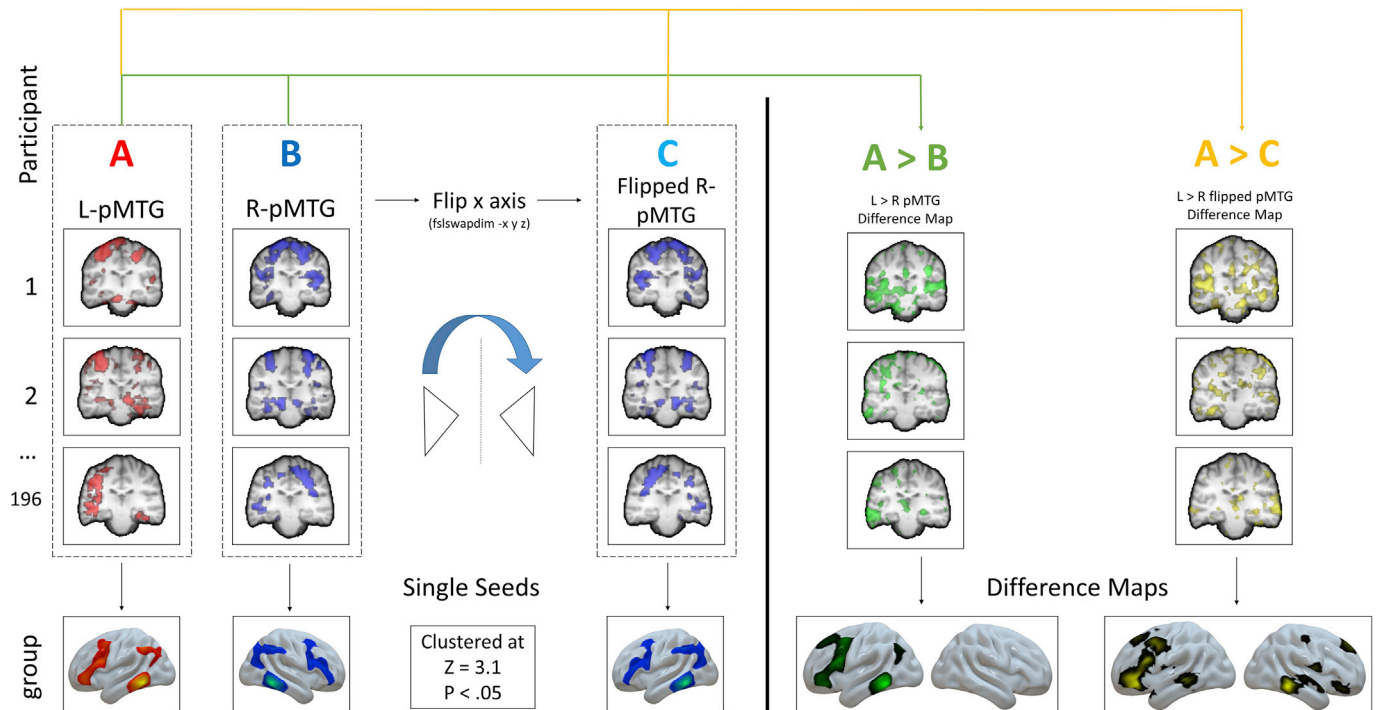

Fig. 2. Analysis pipeline for the single seed correlation analysis and for the difference analyses using posterior middle temporal gyrus as an example. The A and B columns illustrate our single seed analyses, while A > B and A > C show our direct and flipped difference analyses respectively. The green arrow describes our pipeline for the direct comparison difference maps, which highlight the differences in the topography of connectivity for left and right seeds, while the yellow shows the one for the flipped difference maps, which reveal differences in the shape of these topographies for left and right seeds.

Analysis S3 provides the shared connectivity of each LH seed and its RH homotope; these maps are also available on NeuroVault (https://neur ovault.org/collections/4683/).

2.5.6. Cognitive decoding and automated meta-analysis using Neurosynth

Connectivity maps were uploaded to Neurovault (Gorgolewski et al., 2015, https://neurovault.org/collections/4683/) and decoded using Neurosynth (Yarkoni et al., 2011). Neurosynth is an automated meta-analysis tool that uses text-mining approaches to extract terms from neuroimaging articles that typically co-occur with specific peak co-ordinates of activation. It can be used to generate a set of terms frequently associated with a spatial map (as in Figs. 5 and S3). The results of cognitive decoding were rendered as word clouds using R. We manually excluded terms referring to neuroanatomy (e.g., "inferior" or "sulcus"), as well as repeated terms (e.g., "semantic" and "semantics"). The size of each word in the word cloud relates to the frequency of that term across studies.

Neurosynth can also generate 'reverse inference' maps associated with a particular term, such as "semantic". This approach highlights regions that are more likely to be activated for that particular term than for others (as in Fig. 3).

2.5.7. Associations between connectivity and behavioural performance

In a final step, we considered whether individual differences in intrinsic connectivity from our LH seeds correlated with behavioural performance. We elected to focus on LH seeds since all four LH seeds are implicated in semantic processing, while this is not the case for all the RH seeds. This decision also allowed us to avoid the inflation of type I error which would arise from examining many seeds. However, seeding the LH semantic sites still allows us to test the hypothesis that lateralisation of connectivity has functional consequences, since we can consider individual differences in the extent to which these LH seeds couple with other LH semantic and language sites, vs. homologous regions in the RH. We might expect for a highly-lateralised seed like pMTG, connectivity to other LH regions might be associated with good performance, while strong intrinsic connectivity to RH homologues of semantic regions might be associated with poor performance. Since bilateral ATL is implicated in semantic processing, we also examined behavioural associations with right ATL connectivity in a supplementary analysis (following reviewers' comments), but found no significant effects. In each analysis, we included as EVs the efficiency scores corresponding to the four semantic conditions (Weak and Strong associations, Picture and Word modalities of presentation), the non-semantic perceptual matching task as a control, and a motion regressor using the mean (across time/frames) of the absolute values for framewise displacement for each participant. We z-scored the behavioural data, and imputed all outliers exceeding $z > 2.5$ with the cut-off value (except for the motion regressor). The resulting data was mean-centred and entered into a model where we defined as contrasts of interest: group intrinsic connectivity for the seed, semantic > perceptual matching (with semantic performance estimated as the average of the four semantic conditions), weak > strong associations, picture > word modality and the reverse contrasts. Significant clusters were identified using the methods above, with the addition of a Bonferroni correction to account for the one-tailed nature of our tests and the fact that we initially examined four seeds (ATL, AG, IFG, pMTG).[1] We therefore accepted $p = .0063$ ($p = .05/8$) as reaching the threshold for significance. Since the average efficiency scores were significantly different across conditions, we included two extra contrasts to control for difficulty: Given that the weak and strong associations conditions were the hardest and easiest respectively, and the perceptual task was midpoint between the two, we contrasted strong > perceptual and perceptual > weak, to establish if effects could be attributed to difficulty.

---

[1] We did not correct for the additional RH ATL seed, reported in Supplementary Materials, since it was added following the reviewers' comments.

2.6. Data and code availability statement

Neuroimaging data at the group level are openly available in Neurovault at https://neurovault.org/collections/4683/. The conditions of our ethical approval do not permit public archiving of the raw data because participants did not provide sufficient consent. Researchers who wish to access the data and analysis scripts should contact the Research Ethics and Governance Committee of the York Neuroimaging Centre, University of York, or the corresponding author, Beth Jefferies. Data will be released to researchers when this is possible under the terms of the GDPR (General Data Protection Regulation).

3. Results

3.1. Intrinsic connectivity of LH and RH seed regions

Fig. 3 shows the intrinsic connectivity maps for the four LH seeds and their RH homotopes. The connectivity maps and all results discussed in this section can be found in Neurovault (https://neurovault.org/collecti ons/4683/). All LH seeds showed intrinsic connectivity with other left-lateralised semantic regions (i.e. ATL, AG, IFG, pMTG), as well as with their RH homotopes (Fig. 3, rows 2–5). The intrinsic connectivity of these regions showed clear overlap with an automated meta-analysis for the term 'semantic' performed using Neurosynth (row 1). Left ATL showed relatively strong connectivity to other temporal lobe regions and IFG (see Jackson et al., 2016 for similar results – although unlike that study, we did not observe strong intrinsic connectivity between left ATL and dorsomedial prefrontal cortex; see also Supplementary Fig. S1). AG showed strong connectivity to all other semantic seeds and to medial default network regions in posterior cingulate and medial prefrontal cortex. Left pMTG and IFG showed highly similar patterns of connectivity, consistent with the proposal that these brain areas form a distributed network underpinning semantic control. Along with left-lateralised semantic regions, both pMTG and IFG showed strong connectivity to dorsal medial prefrontal cortex, bordering preSMA, and to lateral prefrontal regions in the RH, which are implicated in the control of memory (Noonan et al., 2013).

We next quantified the degree to which patterns of intrinsic connectivity are similar across pairs of seeds implicated in semantic control (IFG and pMTG) or not associated with control (ATL and AG; see Fig. 4). We correlated the intrinsic connectivity of each seed with the three other seeds within the same hemisphere (for example, we compared left IFG-pMTG with left IFG-AG and left IFG-ATL) and tested for significant differences between these correlations using the Fisher r-to-z transformation. Table 2 shows the correlations between all the different pairs of intrinsic connectivity maps.

There was extensive shared connectivity for pMTG and IFG, in both hemispheres. Overlap between IFG and pMTG was seen within these two seed regions, but also within other regions implicated in executive control, such as intraparietal sulcus and pre-supplementary motor area, in both hemispheres (see Fig. 4). The intrinsic connectivity patterns of IFG and pMTG showed higher correlations with each other than with other semantic sites. In both hemispheres, IFG was significantly more correlated with pMTG than with either AG (LH: $z = 7.72$, $p < .001$; RH: $z = 5.33$, $p < .001$) or ATL (LH: $z = 9.57$, $p < .001$; RH: $z = 7.91$, $p < .001$). Likewise, pMTG was more correlated with IFG than with AG (LH: $z = 5.48$, $p < .001$; RH: $z = 3.15$, $p = .002$) and ATL (LH: $z = 7.68$, $p < .001$; RH: $z = 5.01$, $p < .001$). These results demonstrate that the semantic network is not homogeneous: LH sites implicated in semantic control are more connected to each other than to other semantic regions, and the same pattern is seen for their RH homologues.

ATL and AG are not implicated in semantic control and Fig. 4 shows that these sites overlap with DMN sites – including within ATL, medial prefrontal cortex, AG and hippocampus. However, comparisons of the correlations in Table 2 suggest that ATL and AG are not always more connected to each other than to other semantic sites, and in this way,
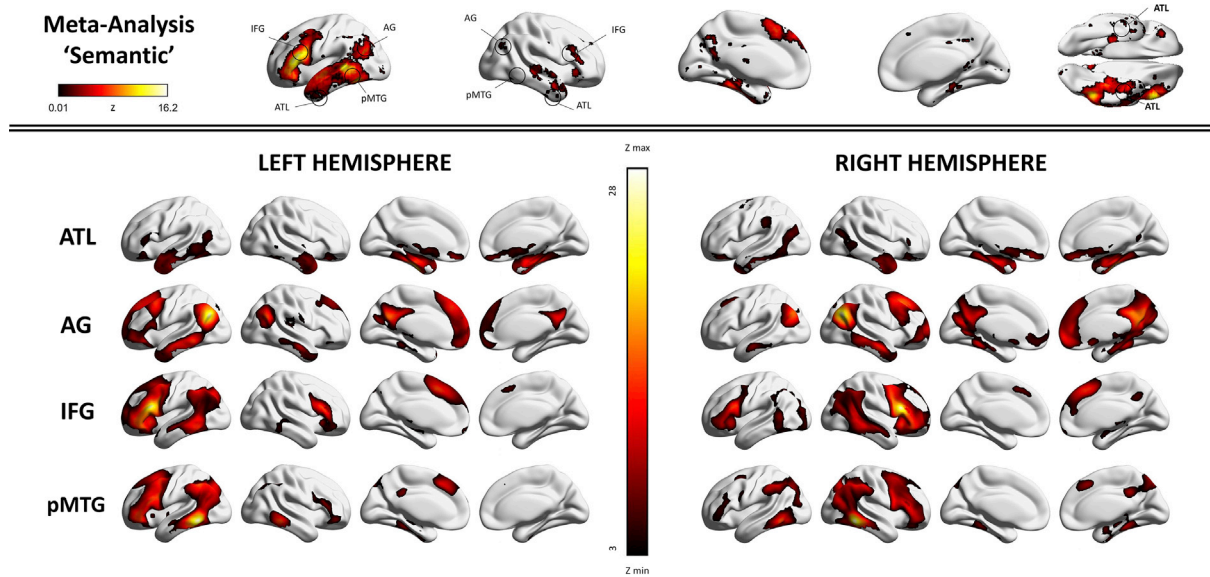
Fig. 3. The top row depicts the meta-analytic map for the term 'semantic' extracted from Neurosynth, with the location of the LH and RH seeds indicated. The bottom panel shows the group mean intrinsic connectivity maps for these LH and RH seeds, projected to the surface using BrainNet. These connectivity maps present Z values (unthresholded).
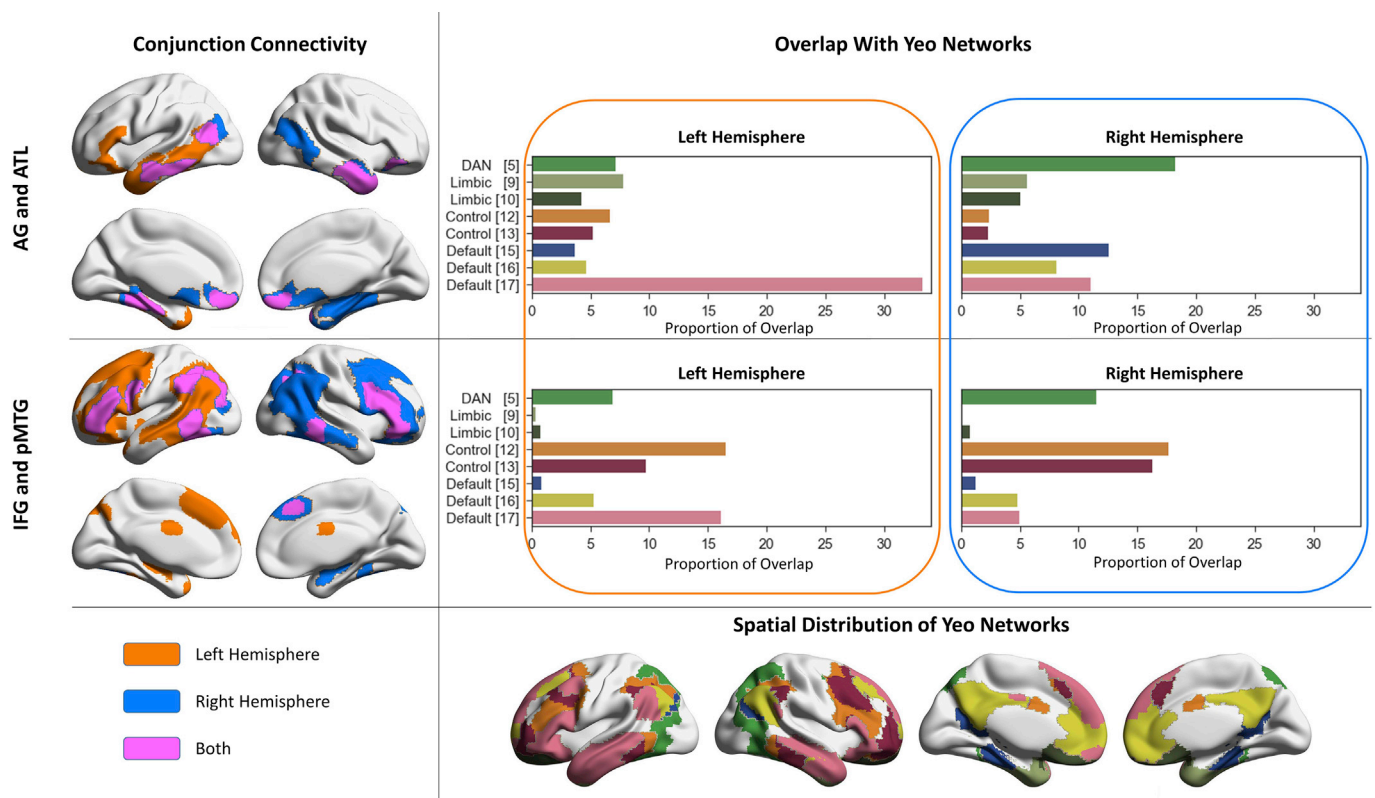

Fig. 4. The maps in the left-hand column depict conjunctions of group mean intrinsic connectivity for pairs of ROIs located in distant parts of cortex (semantic control sites, IFG and pMTG; and sites outside the semantic control network, in AG and ATL). Orange shows regions of overlap between LH seeds while blue shows overlap between RH seeds (pink shows regions of overlap between pairs of semantic seeds that were present for both LH and RH conjunctions). The bar plots adjacent to each conjunction map show the proportion of voxels of this map that overlap with networks from the 17-network parcellation described by Yeo et al. (2011, depicted in the bottom row, colour-coded to match the bar plots; the network names and colour codes for these maps and the corresponding bar plots above can be consulted in detail in Shinn et al., 2015). To simply this figure, we only show those networks for which at least 5% of the voxels in at least one connectivity map showed overlap. Connectivity maps are projected to the surface and plotted using BrainNet.

they do not appear to form a strong sub-network within the semantic system. In the LH, there was a difference between AG-ATL and AG-IFG coupling which approached significance (z = −1.73, p = .08), while in the RH, there was no evidence that AG was more correlated with ATL than IFG (z = −0.58, p > .1). In both hemispheres, AG showed stronger intrinsic connectivity with pMTG (a nearby site) than with ATL (LH:

Table 2
Within-hemisphere correlations for our four ROIs group mean connectivity maps. All correlations are significant at p < .001. Correlations that are different between LH and RH, and those that are not statistically equivalent across hemispheres, are highlighted in bold. The correlations reported here are not corrected for multiple comparisons, although applying Bonferroni correction does not change the outcome.

	LH	RH	LH vs. RH: Fisher r to z	Equivalence test for difference in r (TOST)
IFG to pMTG	.795	.640	**z = 3.21, p = .001**	**r(194) = 0.16, p = .223**
IFG to AG	.293	.212	z = 0.85, p > .1	r(194) = 0.08, p = .036
IFG to ATL	.113	-.047	z = 1.58, p = .1	**r(194) = 0.16, p = .245**
pMTG to AG	.483	.412	z = 0.87, p > .1	r(194) = 0.07, p = .026
pMTG to ATL	.294	.243	z = 0.54, p > .1	r(194) = 0.05, p = .013
ATL to AG	.125	.155	z = −0.30, p > .1	r(194) = -0.03, p = .006
Average intra-hemispheric correlation	.351	.269		

z = −3.94, p = .0001; RH: −2.77, p = .0056). The LH correlation for ATL-AG was not statistically different from ATL-IFG (z = −0.12, p > .1), although in the RH, we found a marginally stronger correlation for ATL-AG than AG-IFG (z = 2.0, p = .05). Finally, there was no evidence that ATL-AG correlations were stronger than ATL-pMTG correlations, in both LH (where there was a trend in the opposite direction; z = −1.74, p = .8) and RH (z = 0.90, p > .1).

In a final step, we compared the patterns of shared connectivity for IFG-pMTG (implicated in semantic control) and for ATL-AG (not implicated in control) in the LH and RH, with canonical networks derived from a parcellation of resting-state connectivity (Yeo et al., 2011, Fig. 4). The left-lateralised semantic control sites (IFG and pMTG) showed a high degree of overlap with both DMN and control networks, supporting the view that these regions sit at the intersection of networks that are typically anti-correlated yet recruited together during semantic tasks (Davey et al., 2016). The RH homologue regions showed a high degree of overlap with control networks (frontoparietal and dorsal attention network) but not with DMN. The connectivity patterns of LH non-control semantic regions (AG and ATL) showed high overlap with lateral default mode regions, not core DMN regions, such as posterior cingulate cortex. The RH homologue regions showed a similar degree of overlap with lateral, core and medial DMN networks, and also strong overlap with the dorsal attention network.

3.2. Similarities and differences in intrinsic connectivity across hemispheres

The left and right hemisphere maps were largely symmetrical (see Fig. 3 and Supplementary Fig. S1). We tested for any significant differences in the strength of the correlation between particular pairs of seeds in the LH and RH using the Fisher r-to-z transformation. We also tested for equivalence between the correlations in each hemisphere using the Two One-Sided Tests (TOST) approach as implemented by Lakens (2017). ATL showed the most symmetrical pattern of connectivity (Pearson's r: ATL = 0.85, AG = 0.46, IFG = 0.43 and pMTG = 0.52, all p < .001): this site had a significantly higher correlation across LH and RH seeds than all of the other sites (using a Fisher to z transform, z > 6.68, p < .001). The strength of cross-hemisphere correlations for the other seeds were not significantly different from each other (z < 1.15, p > .2; all statistically equivalent, p < .05).

We also compared the strength of correlation between different pairs of seeds in LH and RH. The correlation between IFG and pMTG was significantly higher in the LH than the RH (results of analysis shown in Table 2), consistent with the hypothesis that the semantic control system

is particularly left-lateralised. The strength of correlations across other seeds was not significantly different in the LH and RH, and in most cases they were statistically equivalent (with one exception: ATL to IFG showed a numerically higher correlation in the LH, which was not statistically equivalent to RH). All correlations were positive except between IFG and ATL in the RH, which showed a negative correlation.

In summary, the analysis so far shows (i) the semantic system is not homogeneous, with higher similarity between the intrinsic connectivity patterns of the semantic control sites (IFG and pMTG); (ii) ATL shows a more symmetrical pattern of connectivity than other sites, in line with the view this site is a bilateral semantic hub; (iii) the connectivity pattern underpinning the semantic control network is highly lateralised to the LH.

3.3. Differences in network topography between hemispheres

To characterise any differences in the topographical organisation of connectivity from left lateralised semantic regions and their homotopes in RH, we directly contrasted the connectivity of LH and RH for each seed location. In a basic analysis, we computed the simple difference maps between LH and RH seeds. The contrasts of LH > RH and RH > LH produced largely symmetrical maps, which are provided in the Supplementary Materials (Supplementary Analysis S2, Fig. S3). All LH sites showed strong connectivity to semantic sites, while right-lateralised seeds showed strong connectivity to the homotopic sites in the RH (indicated by the symmetry of the red and blue regions). In order to compare the shapes of connectivity patterns directly, we flipped the connectivity map of the RH seeds into LH space, and subtracted one map from the other, to identify regions of stronger and weaker connectivity in LH, relative to the pattern for the RH. For example, a region like left IFG might show stronger intrinsic connectivity to left ATL than would be expected from the pattern of connectivity between right IFG and right ATL. This difference in network topography can be highlighted through a comparison of the connectivity maps for left and right IFG by flipping the RH seed map along the x axis (see Fig. 2, which illustrates this method). The results are shown in Fig. 5. We then compared these connectivity difference maps with the network parcellation provided by Yeo et al. (2011). In Fig. 5, we show differences in network overlap for regions with stronger than expected connectivity to the LH seed given the pattern for the RH seed, and the reverse. Networks overlapping with both L > R and R > L maps to an equal degree fall at the zero point of these charts, since our focus is on network differences.

Left ATL showed stronger connectivity to medial temporal cortex, right ATL, left ventral IFG/insula and left intraparietal sulcus, relative to the connectivity of right ATL flipped into LH space. This is consistent with the low correlation between right ATL and IFG reported above. The right ATL (flipped into LH space) showed stronger connectivity to AG and dorsomedial prefrontal cortex, relative to the pattern of connectivity seen for left ATL. The regions with stronger left-lateralised ATL connectivity showed more extensive overlap with lateral DMN and limbic networks, while the regions with stronger right-lateralised ATL connectivity overlapped to a greater extent with multiple control and attention networks.

Left AG showed stronger connectivity to left and right lateral occipital-temporal cortex, right ATL, left and right IFG, left and right dorsal medial prefrontal cortex and portions of somatomotor cortex, relative to right AG flipped into LH space. The right AG (flipped into LH space) showed stronger connectivity to precuneus and posterior cingulate cortex, plus medial temporal lobe regions. The regions with stronger left-lateralised AG connectivity showed more extensive overlap with lateral DMN and the ventral attention network. The regions with stronger right-lateralised AG connectivity showed greater overlap with visual, control and core/medial DMN networks.

Left IFG showed stronger connectivity to left motor cortex, extending into left dorsal medial prefrontal cortex, and to left inferior frontal cortex. Left pMTG showed a similar pattern, extending further into left IFG, right pMTG and left and right lingual gyrus/cuneus. LH IFG and pMTG seeds
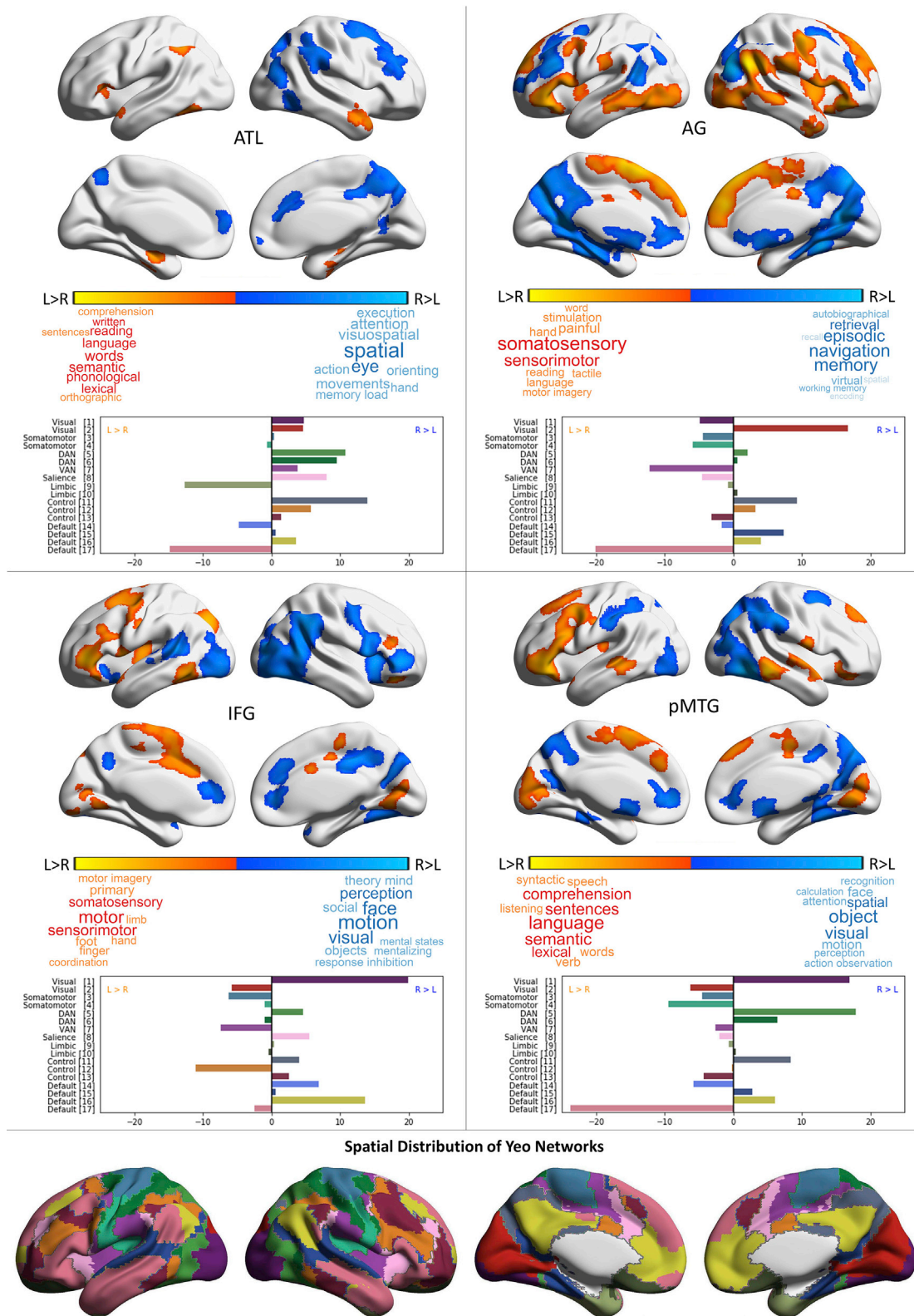
Fig. 5. Intrinsic connectivity group maps showing differences in the network topography (shape/magnitude) of connectivity patterns for left and right hemisphere seeds. The connectivity patterns for right hemisphere seeds were 'flipped' into left hemisphere space, and the maps therefore characterise differences in the shapes and magnitudes of largely symmetrical patterns of connectivity for the two hemispheres (z = 3.1, p < .05); these patterns are depicted in Fig. S3. The results of cognitive decoding using Neurosynth (Yarkoni et al., 2011) are shown in the word clouds below the colour bars. The charts for each seed show a comparison of these spatial maps with the Yeo et al. (2011) 17 networks (depicted in the bottom row, colour-coded to match the bar plots). Each chart plots the difference in overlap for each network from Yeo et al., comparing the LH > RH and RH > LH connectivity maps. A left-facing bar corresponds to more extensive overlap with the left-lateralised connectivity map, while a right-facing bar corresponds to more extensive overlap with the right-lateralised connectivity map. The network names and colour codes are taken from Shinn et al. (2015).

also showed weaker connectivity to parietal-occipital fissure, intra-parietal sulcus, precuneus, posterior cingulate and medial prefrontal cortex, both within and across hemispheres, compared with right-hemisphere seeds (indicated by the presence of blue in Fig. 5). Regions with stronger left-lateralised IFG connectivity showed more extensive overlap with control, ventral attention, medial visual and somatomotor networks, while sites with more right-lateralised IFG connectivity showed greater overlap with core DMN and lateral visual regions. Regions with stronger left-lateralised pMTG connectivity showed greater overlap with lateral DMN, while sites with more right-lateralised pMTG connectivity showed greater overlap with dorsal attention and lateral visual networks.

We applied cognitive decoding to these maps using Neurosynth (see word clouds in Fig. 5). The set of brain regions showing stronger connectivity with LH seeds were associated with semantic and language

terms (pMTG and ATL) and somatomotor processing (for IFG and AG). Brain regions showing stronger connectivity to RH seeds were associated with terms relating to visual-spatial processing. This association between left-lateralised connectivity and somatomotor processing as well as semantics and language has previously been reported by Gotts et al. (2013). To quantify these differences, we obtained meta-analytic maps from Neurosynth for key terms thought to show strong lateralisation (terms with presumed LH lateralisation: semantic, language, words; terms with presumed RH lateralisation: visual, spatial, attention) and we computed their correlation with our connectivity difference maps. We found that brain regions showing stronger connectivity with LH seeds had positive correlations with these left-lateralised terms (average for the four seeds: r = 0.13) and negative correlations with right-lateralised terms (average: r = −0.11); the reverse was true for regions with stronger connectivity to RH seeds (average correlation with right lateralised terms: r = 0.1; with
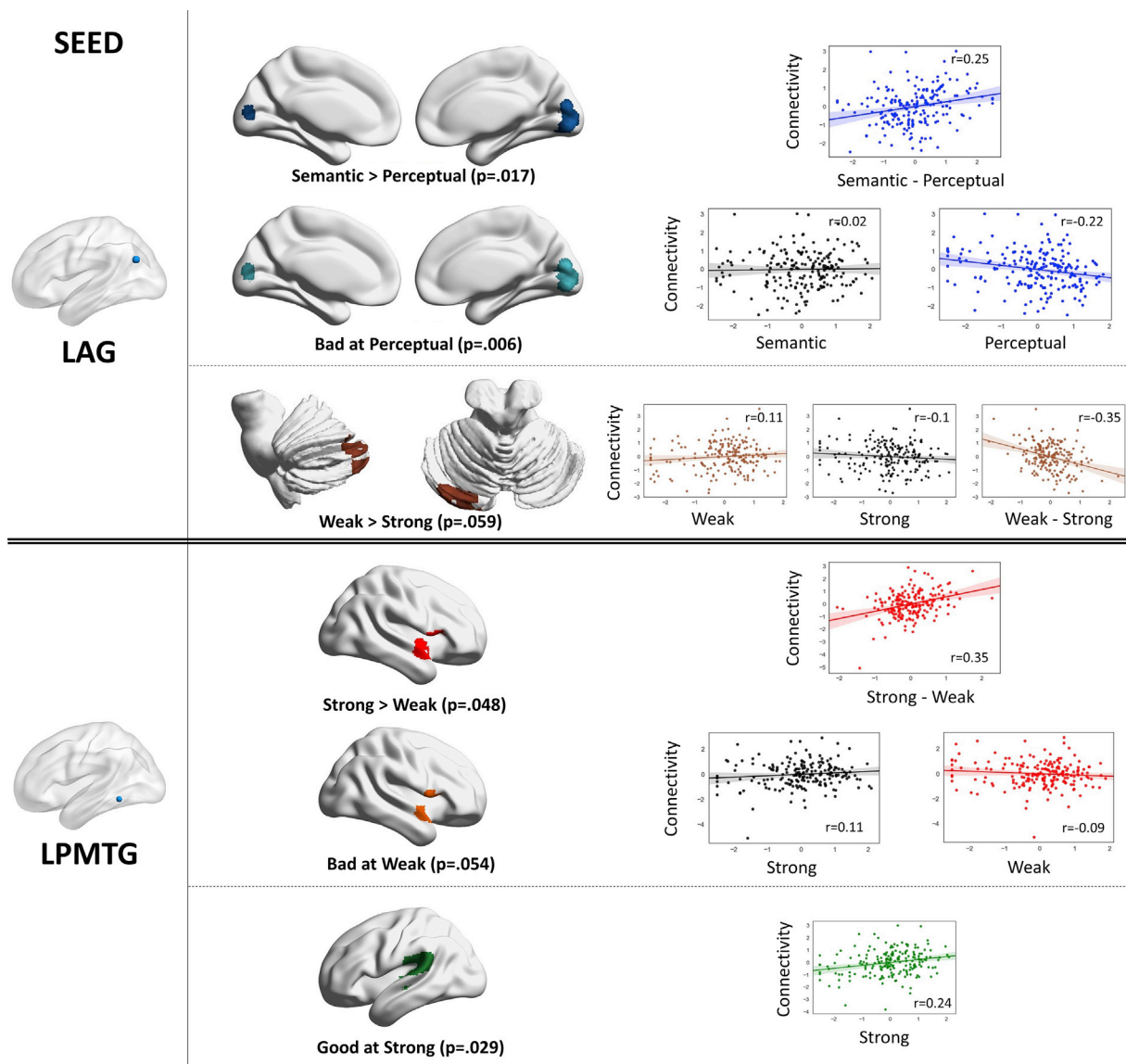

Fig. 6. Regions associated with behavioural performance in semantic tasks as a function of their connectivity with left angular gyrus and posterior middle temporal gyrus. The scatterplots show the mean connectivity of the seed to the cluster for each participant as a function of their behavioural efficiency score in the task condition depicted in the brain images. The top panel shows results by type of stimulus, and the bottom panel by strength of association. We found no significant results for ATL and IFG. The results were projected to the surface and displayed using SurfIce for ease of viewing (non-projected results can be seen in Neurovault: https://neurovault.org/collections/4683/and their peaks can be consulted in Table 4). The scatterplots were produced using FSL's featquery to extract the mean strength of connectivity between the seed and cluster. The effects survived Bonferroni correction for four seeds and the two-way nature of our tests, with the exception of the AG-cerebellar cluster (p = .059) and the pMTG-right aSTG cluster for the main effect of poor weak associations (p = .054). The p values in the figure are Bonferroni corrected for 8 multiple comparisons.

left-lateralised terms: r = −0.14). These findings are consistent with the view that different patterns of connectivity from homotopic regions in left and right hemisphere relate to functional distinctions observed in neuropsychological investigations (where spatial neglect is more associated with right-lateralised lesions, and semantic-language dysfunction with left-lateralised lesions).

3.4. Intrinsic connectivity of semantic seeds regions predicts behavioural efficiency

We analysed the behavioural results of our tasks using repeated-measures ANOVAs with Greenhouse-Geisser correction to test for significant differences between conditions. There was an effect of condition for both accuracy (F(2.92, 574.24) = 303.33, p = .000) and RT (F(2.74, 540.08) = 420.85, p = .000). Speed and accuracy may be traded off in different ways across tasks and individuals. We overcame this issue by using inverse response efficiency to capture global performance (RT divided by accuracy, multiplied by −1; high scores reflect good performance). We have successfully used this approach in other recent studies (Gonzalez Alam et al., 2018; Lanzoni et al., 2019; Murphy et al., 2018; Poerio et al., 2017; Vatansever et al., 2017; H. T. Wang et al., 2018b; X. Wang et al., 2018). There was a difference in response efficiency across conditions (F(2.64, 519.45) = 398.05, p = .000). Bonferroni corrected t-tests revealed participants were less efficient for weak than strong associations (t(195) = 30.02, p = .000), and less efficient for word than picture decisions (t(195) = 17.95, p = .000). Participants were also more efficient in three of the four semantic tasks relative to perceptual judgements (t(195) = 5.58–19.01, p = .000), yet less efficient for weak associations relative to perceptual trials (t(195) = 10.28, p = .000).

We examined the relationship between the intrinsic connectivity of each of our four LH ROIs and task performance outside the scanner, to test the hypothesis that stronger connectivity *within* LH cortical regions is associated with efficient semantic retrieval, while stronger connectivity *between* LH seeds and RH regions disrupts semantic control. The results are summarised in Fig. 6. Supplementary analyses to confirm that these effects did not solely reflect differences in task difficulty are shown in Table 3.

We found a significant relationship between the strength of intrinsic connectivity of two semantic seeds – AG and pMTG – and individual differences in participants' efficiency when performing semantic and perceptual tasks, in whole-brain analyses. Connectivity from left AG to bilateral medial occipital regions was associated with differential performance on perceptual and semantic tasks (Fig. 6; dark blue). Participants with poorer performance on perceptual decisions, relative to semantic decisions, showed stronger connectivity from left AG to bilateral occipital cortex. An overlapping cluster predicted weak performance on perceptual trials (Fig. 6; light blue). Since the perceptual decisions were more difficult than the semantic decisions overall, it is possible that this contrast reflected poorer performance on harder decisions in general, in participants with weaker connectivity from left AG to occipital cortex. As a control analysis, we compared weak associations (a harder semantic task) with perceptual matching and found the same positive correlation, suggesting that irrespective of difficulty, participants with poorer perceptual than semantic performance have stronger connectivity from

left AG to occipital cortex.

Patterns of connectivity from pMTG – a key semantic control site – also predicted the capacity to retrieve weak associations, relative to strong associations, and therefore the retrieval of non-dominant aspects of knowledge in a controlled fashion to suit the circumstances. Stronger within-hemisphere coupling to left pSTG and supramarginal gyrus, implicated in language (Fig. 6, green), was associated with the efficient retrieval of strong associations. In contrast, cross-hemisphere connectivity with right aSTG was associated with poorer performance on weak relative to strong associations (Fig. 6, red and orange). Since weak associations are harder than strong associations, we performed a supplementary analysis to test the effect of this cross-hemispheric connectivity pattern on demanding tasks in general. There was no correlation between this pattern of connectivity (defined by the strong vs. weak association contrast) and performance on easy semantic vs. harder perceptual decisions, suggesting that the association between connectivity and performance was specific to demanding semantic judgements.

There was an additional effect which did not survive Bonferroni correction. AG's connectivity to a left cerebellar cluster (Fig. 6, brown) was positively associated with participants' efficiency in retrieving weak associations (relative to strong associations), consistent with a role for the cerebellum in semantic cognition. No patterns of connectivity predicted differences between word and picture performance. This null result perhaps reflects the heteromodal nature of the seeds we selected. Finally, in order to increase our confidence that the results obtained were not specific to a particular cluster-forming threshold, we conducted additional analyses using Threshold-Free Cluster Enhancement (Smith and Nichols, 2009). All of the results shown in Fig. 6 replicated for 5000 permutations. Full results from this supplementary analysis are provided in NeuroVault (https://neurovault.org/collections/4683/).

In summary, when connectivity from left pMTG to other LH language regions is relatively strong, participants tend to be good at retrieving strong associations. In contrast, when this region shows stronger connectivity to RH homologues of semantic processing, the retrieval of weak associations is less efficient. These results are consistent with the view that the semantic control system is strongly left-lateralised. We also found that when left AG has stronger intrinsic connectivity to visual cortex, participants tend to perform perceptual judgements less efficiently, suggesting that semantic and perceptual information might compete for processing in left AG.

4. Discussion

This study characterised similarities and differences in intrinsic connectivity between LH sites implicated in semantic cognition, and their RH homotopes, and explored the functional significance of individual differences in these connectivity patterns. Since distinct neurocognitive components are thought to underpin semantic representation and control processes, we focussed on whether there are differences in the lateralisation of these components. We found that intrinsic connectivity analyses were consistent with the view that the semantic system is not homogeneous: sites implicated in semantic control – IFG and pMTG – were more strongly connected to each other than they were to other semantic sites (ATL and AG). The semantic control network was also strongly left-lateralised, since the connectivity between IFG and pMTG was stronger in the LH than RH – and this lateralisation in connectivity was unique to this pair of seeds. Conversely, ventral ATL implicated in semantic representation showed the most symmetrical connectivity, consistent with the view that this site is a bilateral 'hub'. Cognitive decoding of differences in the topology of connectivity across LH and RH found semantic, language and motor terms for LH semantic seeds, and terms related to visual attention, spatial processing and navigation for RH seeds, suggesting that distinct patterns of connectivity across the hemispheres relates to the lateralisation of semantic cognition in the LH, and potentially the right lateralised nature of other functions such as spatial attention.

Individual differences in intrinsic connectivity also predicted task

Table 3
Correlations to control for possible difficulty confounds in our behavioural regressions. In these supplementary analyses, we took patterns of connectivity defined by the main analysis and computed correlations with different task effects.

Seed	Connectivity to:	Behavioural control	r	p
pMTG	Strong > Weak (RH)	Strong - Perceptual	0.04	0.62
AG	Weak > Strong (Cerebellum)	Weak - Perceptual	0.09	0.2
	Semantic > Perceptual (Occipital)	Weak - Perceptual	0.91	<0.001

Table 4
Peak coordinates for behavioural regression results. p values are reported after applying Bonferroni correction for 8 multiple comparisons (to account for 4 seed regions and the two-tailed nature of our tests). For completeness, all results where p < .1 are shown, including two non-significant results. The coordinates are given in MNI (mm) and the labels were obtained from the Harvard-Oxford Cortical Structural Atlas and Cerebellar Atlas in MNI152 space after normalisation with FLIRT. Full maps are provided on Neurovault (https://neurovault.org/collections/4683/).

Seed	Contrast	Hemisphere	Connectivity	Voxels	p	Peak Z	x	y	z
AG	Semantic > Perceptual	Left	Lingual Gyrus	497	.018	4.2	12	−86	−4
	Bad at Perceptual	Left	Lingual Gyrus	606	.006	4.2	12	−86	−4
	Weak > Strong	Left	Cerebellum Crus I	380	.059, n.s	4.27	−36	−78	−26
pMTG	Strong > Weak	Right	Planum Polare	396	.048	4.94	46	0	−8
	Bad at Weak	Right	Planum Polare	385	.054, n.s	4.63	46	0	−8
	Good at Strong	Left	Parietal Operculum	443	.029	4.96	−54	−34	20

performance: participants who had stronger connectivity between left pMTG and LH regions tended to have more efficient retrieval of strong associations. Conversely, stronger connectivity from left pMTG to right IFG/aSTG (homologous to the LH conjunction site) was related to poorer controlled retrieval of weak associations. This finding is consistent with the view that left-lateralised connectivity within the semantic control network is associated with better semantic control. We also found that when left AG was more connected to visual cortex, people were poorer at perceptual tasks. Left AG is implicated in semantic retrieval and understanding meaningful conceptual combinations (Davey et al., 2015; Humphreys and Lambon Ralph, 2015; Murphy et al., 2018). More widely, inferior parietal cortex is implicated in stimulus-driven visual attention, as well as reflexive attention to memory (Cabeza et al., 2008) and multimodal feature integration in memory (Bonnici et al., 2016). Consequently, there may be individual differences that reflect a trade-off between perceptual and memory-based cognition in AG (see also Sormaz et al., 2017). When this site in the LH connects more to visual regions that are allied to right-lateralised patterns of connectivity, the network implicated in visual attention (e.g. by cognitive decoding) may be weakened. There was one further behavioural regression effect – stronger connectivity from AG to a left cerebellar cluster, which predicted better semantic control – however, this effect did not pass Bonferroni correction for the number of analyses. Since cerebellar lateralisation is opposite to that in the cortex, this result could indicate that semantic control is better in people with less lateralised connectivity from AG. This pattern would potentially give rise to a left-lateralised semantic network that is more strongly dominated by semantic control regions, and less dominated by DMN. However, the evidence for this pattern was weak and it requires replication.

Our methodology, which compared patterns of intrinsic connectivity from LH seeds and RH seeds flipped into LH space, resembles the approach of Raemaekers et al. (2018). This recent study found that resting-state connectivity was symmetrical in around 95% of regions, yet asymmetrical in language regions, and this predicted the BOLD response to a story versus a maths task (see also Gotts et al., 2013; Hurley et al., 2015; Jo et al., 2012; Karolis et al., 2019; Raemaekers et al., 2018; Wang et al., 2014). The current study adds to this body of work by specifically assessing connectivity differences for four key heteromodal semantic nodes, as opposed to language sites, and by differentiating between sites implicated in heteromodal conceptual representation (ventral ATL) and semantic control (IFG; pMTG). We found strong left-lateralisation similar to that reported by Raemaekers et al. (2018) for semantic control sites, but not for ventral ATL. Moreover, we used a fine-grained semantic battery examining different modalities (words; pictures) and semantic control demands (strong vs. weak associations). As well as stronger lateralisation of intrinsic connectivity for the semantic control sites in resting-state fMRI, we found poor controlled retrieval of weak associations was associated with more right-lateralised connectivity from a key LH site implicated in semantic control. However, we did not observe differences between verbal and non-verbal tasks, potentially consistent with the heteromodal nature of our seeds.

These findings fit broadly with several key predictions of the

Controlled Semantic Cognition framework. According to this theory, semantic representation draws on a semantic 'hub' in bilateral ATL, with some relatively subtle functional specialisation for verbal and non-verbal semantic tasks in left and right ATL respectively (Rice et al., 2018a, 2015a; 2015b). We found highly symmetrical connectivity maps for left and right ventral ATL, in line with other recent studies (Jackson et al., 2017). We found no evidence that connectivity patterns from left ATL were associated with different performance on word and picture matching tasks – although we cannot rule out the possibility that connectivity patterns from left and right ATL would differentially predict performance on tests requiring specific identities to be retrieved, such as names and faces (Rice et al., 2018a, 2015b; 2015a). The CSC framework envisages that semantic representations (supported by the ATL hub interacting with sensory-motor spokes) are shaped by control processes supported by a different network, including IFG and pMTG. It is interesting to speculate about why semantic activation is left-lateralised, given that ATL is assumed to represent concepts bilaterally. Given the CSC framework proposes at least two interacting components – namely bilateral semantic representations and control processes – we might anticipate that the semantic control system is the most lateralised component, but this prediction has rarely if ever been tested. We found evidence for a lateralised semantic control network both in terms of patterns of intrinsic connectivity at rest and lateralisation predicting behavioural performance on weak vs. strong associations.

The patterns we observed may be explicable in terms of different interactions between large-scale networks in LH semantic regions, relative to their RH counterparts. The frontoparietal network is the most segregated network across the hemispheres, coupling more to DMN in LH and more to attention networks in RH (Dixon et al., 2018; Wang et al., 2014). For our two heteromodal semantic seeds which showed relatively high connectivity to FPN regions (IFG; pMTG), there appeared to be greater connectivity to LH lateral DMN regions than would be expected from intrinsic connectivity in the RH (particularly in LH lateral DMN). Moreover, for our semantic DMN seeds in LH (AG; ATL), there was greater connectivity to ventral LOC and anterior insula sites implicated in attention/control. These findings are consistent with Davey et al., (2016) proposal that semantic cognition in the LH involves the integration of DMN and executive networks. One interesting observation is that the conjunction of the intrinsic connectivity maps of all four LH semantic seeds showed strong connectivity to the lateral regions of DMN, which have been previously implicated in semantic cognition – regions such as lateral temporal cortex and angular gyrus – and weak connectivity to medial default mode regions, such as posterior cingulate cortex, medial prefrontal cortex and hippocampus, which are not strongly implicated in semantic cognition. In contrast, the RH seed conjunction showed stronger connectivity to medial core default mode regions. Consequently, lateralised patterns of connectivity that support semantic cognition may reflect a particular form of interaction between DMN and control regions (Davey et al., 2016; Dixon et al., 2018; Wang et al., 2014), and this pattern of interaction might play an important role in functional subdivisions within DMN (e.g. Andrews-Hanna et al., 2010).

Funding

EJ was supported by European Research Council [FLEXSEM-771863], JS was supported by European Research Council [WANDERINGMINDS-646927], TGA was supported by the National Council of Science and Technology, Mexico [Scholarship 411361].

Declarations of interest

None.

Appendix A. Supplementary data

Supplementary data to this article can be found online at https://doi.org/10.1016/j.neuroimage.2019.116089.

References

Andrews-Hanna, J.R., Reidler, J.S., Sepulcre, J., Poulin, R., Buckner, R.L., 2010. Functional-anatomic fractionation of the brain's default network. Neuron 65, 550–562. https://doi.org/10.1016/j.neuron.2010.02.005.

Baciu, M., Juphard, A., Cousin, E., Le Bas, J.F., 2005. Evaluating fMRI methods for assessing hemispheric language dominance in healthy subjects. Eur. J. Radiol. 55, 209–218. https://doi.org/10.1016/j.ejrad.2004.11.004.

Badre, D., Poldrack, R.A., Paré-Blagoev, E.J., Insler, R.Z., Wagner, A.D., 2005. Dissociable controlled retrieval and generalized selection mechanisms in ventrolateral prefrontal cortex. Neuron 47, 907–918. https://doi.org/10.1016/j.neuron.2005.07.023.

Beckmann, C.F., Jenkinson, M., Smith, S.M., 2003. General multilevel linear modeling for group analysis in FMRI. Neuroimage 20, 1052–1063. https://doi.org/10.1016/S1053-8119(03)00435-X.

Behzadi, Y., Restom, K., Liau, J., Liu, T.T., 2007. A component based noise correction method (CompCor) for BOLD and perfusion based fMRI. Neuroimage 37, 90–101. https://doi.org/10.1016/j.neuroimage.2007.04.042.

Bellana, B., Liu, Z., Anderson, J.A.E., Moscovitch, M., Grady, C.L., 2016. Laterality effects in functional connectivity of the angular gyrus during rest and episodic retrieval. Neuropsychologia 80, 24–34. https://doi.org/10.1016/j.neuropsychologia.2015.11.004.

Bemis, D.K., Pylkkänen, L., 2013. Basic linguistic composition recruits the left anterior temporal lobe and left angular gyrus during both listening and reading. Cerebr. Cortex 23, 1859–1873. https://doi.org/10.1093/cercor/bhs170.

Binder, J.R., Desai, R.H., Graves, W.W., Conant, L.L., 2009. Where is the semantic system? A critical review and meta-analysis of 120 functional neuroimaging studies. Cerebr. Cortex 19, 2767–2796. https://doi.org/10.1093/cercor/bhp055.

Bonnici, H.M., Richter, F.R., Yazar, Y., Simons, J.S., 2016. Multimodal feature integration in the angular gyrus during episodic and semantic retrieval. J. Neurosci. 36, 5462–5471. https://doi.org/10.1523/JNEUROSCI.4310-15.2016.

Cabeza, R., Ciaramelli, E., Olson, I.R., Moscovitch, M., 2008. The parietal cortex and episodic memory: an attentional account. Nat. Rev. Neurosci. 9, 613–625. https://doi.org/10.1038/nrn2459.

Chiou, R., Humphreys, G.F., Jung, J., Lambon Ralph, M.A., 2018. Controlled Semantic Cognition Relies upon Dynamic and Flexible Interactions between the Executive 'semantic Control' and Hub-And-Spoke 'semantic Representation' Systems, Cortex. Elsevier Ltd. https://doi.org/10.1016/j.cortex.2018.02.018.

Coltheart, M., 1981. The MRC psycholinguistic database. Q. J. Exp. Psychol. Sect. A 33, 497–505. https://doi.org/10.1080/14640748108400805.

Davey, J., Cornelissen, P.L., Thompson, H.E., Sonkusare, S., Hallam, G., Smallwood, J., Jefferies, E., 2015. Automatic and controlled semantic retrieval: TMS reveals distinct contributions of posterior middle temporal gyrus and angular gyrus. J. Neurosci. 35, 15230–15239. https://doi.org/10.1523/JNEUROSCI.4705-14.2015.

Davey, J., Thompson, H.E., Hallam, G., Karapanagiotidis, T., Murphy, C., De Caso, I., Krieger-Redwood, K., Bernhardt, B.C., Smallwood, J., Jefferies, E., 2016. Exploring the role of the posterior middle temporal gyrus in semantic cognition: integration of anterior temporal lobe with executive processes. Neuroimage 137, 165–177. https://doi.org/10.1016/j.neuroimage.2016.05.051.

Dixon, M.L., De La Vega, A., Mills, C., Andrews-Hanna, J., Spreng, R.N., Cole, M.W., Christoff, K., 2018. Heterogeneity within the frontoparietal control network and its relationship to the default and dorsal attention networks. Proc. Natl. Acad. Sci. 115, E1598–E1607. https://doi.org/10.1073/pnas.1715766115.

Eklund, A., Nichols, T.E., Knutsson, H., 2016. Cluster failure: why fMRI inferences for spatial extent have inflated false-positive rates. Proc. Natl. Acad. Sci. 201602413. https://doi.org/10.1073/pnas.1602413113.

Gonzalez Alam, T., Murphy, C., Smallwood, J., Jefferies, E., 2018. Meaningful inhibition: exploring the role of meaning and modality in response inhibition. Neuroimage 181, 108–119. https://doi.org/10.1016/j.neuroimage.2018.06.074.

Gorgolewski, K.J., Varoquaux, G., Rivera, G., Schwarz, Y., Ghosh, S.S., Maumet, C., Sochat, V.V., Nichols, T.E., Poldrack, R.A., Poline, J.-B., Yarkoni, T., Margulies, D.S., 2015. NeuroVault.org: a web-based repository for collecting and sharing unthresholded statistical maps of the human brain. Front. Neuroinf. 9, 1–9. https://doi.org/10.3389/fninf.2015.00008.

Gotts, S.J., Jo, H.J., Wallace, G.L., Saad, Z.S., Cox, R.W., Martin, A., 2013. Two distinct forms of functional lateralization in the human brain. Proc. Natl. Acad. Sci. U. S. A. 110, E3435–E3444. https://doi.org/10.1073/pnas.1302581110.

Hallam, G.P., Thompson, H.E., Hymers, M., Millman, R.E., Rodd, J.M., Lambon Ralph, M.A., Smallwood, J., Jefferies, E., 2018. Task-based and resting-state fMRI reveal compensatory network changes following damage to left inferior frontal gyrus. Cortex 99, 150–165. https://doi.org/10.1016/j.cortex.2017.10.004.

Hallam, G.P., Whitney, C., Hymers, M., Gouws, A.D., Jefferies, E., 2016. Charting the effects of TMS with fMRI: modulation of cortical recruitment within the distributed network supporting semantic control. Neuropsychologia 93, 40–52. https://doi.org/10.1016/j.neuropsychologia.2016.09.012.

Hoffman, P., McClelland, J.L., Lambon-Ralph, M.A., 2018. Concepts, control, and context: A connectionist account of normal and disordered semantic cognition. Psychol. Rev. 125 (3), 293–328. https://doi.org/10.1037/rev0000094.

Humphreys, G.F., Hoffman, P., Visser, M., Binney, R.J., Lambon Ralph, M.A., 2015. Establishing task- and modality-dependent dissociations between the semantic and default mode networks. Proc. Natl. Acad. Sci. 112, 7857–7862. https://doi.org/10.1073/pnas.1422760112.

Humphreys, G.F., Lambon Ralph, M.A., 2015. Fusion and fission of cognitive functions in the human parietal cortex. Cerebr. Cortex 25, 3547–3560. https://doi.org/10.1093/cercor/bhu198.

Hurley, R.S., Bonakdarpour, B., Wang, X., Mesulam, M.-M., 2015. Asymmetric connectivity between the anterior temporal lobe and the language network. J. Cogn. Neurosci. 27, 464–473. https://doi.org/10.1162/jocn.

Jackson, R.L., Bajada, C.J., Rice, G.E., Cloutman, L.L., Lambon Ralph, M.A., 2017. An emergent functional parcellation of the temporal cortex. Neuroimage 1–15. https://doi.org/10.1016/j.neuroimage.2017.04.024.

Jackson, R.L., Cloutman, L.L., Lambon Ralph, M.A., 2019. Exploring distinct default mode and semantic networks using a systematic ICA approach. Cortex 113, 279–297. https://doi.org/10.1016/j.cortex.2018.12.019.

Jackson, R.L., Hoffman, P., Pobric, G., Lambon Ralph, M.A., 2016. The semantic network at work and rest: differential connectivity of anterior temporal lobe subregions. J. Neurosci. 36, 1490–1501. https://doi.org/10.1523/JNEUROSCI.2999-15.2016.

Jefferies, E., 2013. The neural basis of semantic cognition: converging evidence from neuropsychology, neuroimaging and TMS. Cortex 49, 611–625. https://doi.org/10.1016/j.cortex.2012.10.008.

Jefferies, E., Lambon Ralph, M.A., 2006. Semantic impairment in stroke aphasia versus semantic dementia: a case-series comparison. Brain 129, 2132–2147. https://doi.org/10.1093/brain/awl153.

Jenkinson, M., Bannister, P., Brady, M., Smith, S., 2002. Improved optimization for the robust and accurate linear registration and motion correction of brain images. Neuroimage 17, 825–841. https://doi.org/10.1016/S1053-8119(02)91132-8.

Jenkinson, M., Smith, S., 2001. A global optimisation method for robust affine registration of brain images. Med. Image Anal. 5, 143–156. https://doi.org/10.1016/S1361-8415(01)00036-6.

Jo, H.J., Saad, Z.S., Gotts, S.J., Martin, A., Cox, R.W., 2012. Quantifying agreement between anatomical and functional interhemispheric correspondences in the resting brain. PLoS One 7. https://doi.org/10.1371/journal.pone.0048847.

Karapanagiotidis, T., Bernhardt, B.C., Jefferies, E., Smallwood, J., 2017. Tracking thoughts: exploring the neural architecture of mental time travel during mind-wandering. Neuroimage 147, 272–281. https://doi.org/10.1016/j.neuroimage.2016.12.031.

Karolis, V.R., Corbetta, M., Thiebaut de Schotten, M., 2019. The architecture of functional lateralisation and its relationship to callosal connectivity in the human brain. Nat. Commun. 10, 1417. https://doi.org/10.1038/s41467-019-09344-1.

Krieger-Redwood, K., Teige, C., Davey, J., Hymers, M., Jefferies, E., 2015. Conceptual control across modalities: graded specialisation for pictures and words in inferior frontal and posterior temporal cortex. Neuropsychologia 76, 92–107. https://doi.org/10.1016/j.neuropsychologia.2015.02.030.

Lakens, D., 2017. Equivalence tests. Soc. Psychol. Personal. Sci. 8, 355–362. https://doi.org/10.1177/1948550617697177.

Lambon Ralph, M.A., Cipolotti, L., Manes, F., Patterson, K., 2010. Taking both sides: do unilateral anterior temporal lobe lesions disrupt semantic memory? Brain 133, 3243–3255. https://doi.org/10.1093/brain/awq264.

Lambon Ralph, M.A., Jefferies, E., Patterson, K., Rogers, T.T., 2017. The neural and computational bases of semantic cognition. Nat. Rev. Neurosci. 18, 42–55. https://doi.org/10.1038/nrn.2016.150.

Lambon Ralph, M.A., McClelland, J.L., Patterson, K., Galton, C.J., Hodges, J.R., 2001. No right to speak? The relationship between object naming and semantic impairment: neuropsychological evidence and a computational model. J. Cogn. Neurosci. 13, 341–356. https://doi.org/10.1162/08989290151137395.

Lanzoni, L., Thompson, H., Beintari, D., Berwick, K., Demnitz-King, H., Raspin, H., Taha, M., Stampacchia, S., Smallwood, J., Jefferies, E., 2019. Emotion and location cues bias conceptual retrieval in people with deficient semantic control. Neuropsychologia 131, 294–305. https://doi.org/10.1016/j.neuropsychologia.2019.05.030.

Mion, M., Patterson, K., Acosta-Cabronero, J., Pengas, G., Izquierdo-Garcia, D., Hong, Y.T., Fryer, T.D., Williams, G.B., Hodges, J.R., Nestor, P.J., 2010. What the left and right anterior fusiform gyri tell us about semantic memory. Brain 133, 3256–3268. https://doi.org/10.1093/brain/awq272.

Murphy, C., Jefferies, E., Rueschemeyer, S.-A., Sormaz, M., Wang, H., Margulies, D.S., Smallwood, J., 2018. Distant from input: evidence of regions within the default mode network supporting perceptually-decoupled and conceptually-guided cognition. Neuroimage 171, 393–401. https://doi.org/10.1016/j.neuroimage.2018.01.017.

Murphy, K., Birn, R.M., Handwerker, D.A., Jones, T.B., Bandettini, P.A., 2009. The impact of global signal regression on resting state correlations: are anti-correlated networks

introduced? Neuroimage 44, 893–905. https://doi.org/10.1016/j.neuroimage.2008.09.036.

Noonan, K.A., Jefferies, E., Visser, M., Lambon Ralph, M.A., 2013. Going beyond inferior prefrontal involvement in semantic control: evidence for the additional contribution of dorsal angular gyrus and posterior middle temporal cortex. J. Cogn. Neurosci. 25, 1824–1850. https://doi.org/10.1162/jocn.

Noppeney, U., Phillips, J., Price, C., 2004. The neural areas that control the retrieval and selection of semantics. Neuropsychologia 42, 1269–1280. https://doi.org/10.1016/j.neuropsychologia.2003.12.014.

Patterson, K., Nestor, P.J., Rogers, T.T., 2007. Where do you know what you know? The representation of semantic knowledge in the human brain. Nat. Rev. Neurosci. 8, 976–987. https://doi.org/10.1038/nrn2277.

Poerio, G.L., Sormaz, M., Wang, H.T., Margulies, D., Jefferies, E., Smallwood, J., 2017. The role of the default mode network in component processes underlying the wandering mind. Soc. Cogn. Affect. Neurosci. 12, 1047–1062. https://doi.org/10.1093/scan/nsx041.

Price, A.R., Bonner, M.F., Peelle, J.E., Grossman, M., 2015. Converging evidence for the neuroanatomic basis of combinatorial semantics in the angular gyrus. J. Neurosci. 35, 3276–3284. https://doi.org/10.1523/JNEUROSCI.3446-14.2015.

Raemaekers, M., Schellekens, W., Petridou, N., Ramsey, N.F., 2018. Knowing left from right: asymmetric functional connectivity during resting state. Brain Struct. Funct. 223, 1909–1922. https://doi.org/10.1007/s00429-017-1604-y.

Reilly, J., Peelle, J.E., Garcia, A., Crutch, S.J., 2016. Linking somatic and symbolic representation in semantic memory: the dynamic multilevel reactivation framework. Psychon. Bull. Rev. 23, 1002–1014. https://doi.org/10.3758/s13423-015-0824-5.

Rice, G.E., Caswell, H., Moore, P., Hoffman, P., Lambon Ralph, M.A., 2018a. The roles of left versus right anterior temporal lobes in semantic memory: a neuropsychological comparison of postsurgical temporal lobe epilepsy patients. Cerebr. Cortex 28, 1487–1501. https://doi.org/10.1093/cercor/bhx362.

Rice, G.E., Hoffman, P., Binney, R.J., Lambon Ralph, M.A., 2018b. Concrete versus abstract forms of social concept: an fMRI comparison of knowledge about people versus social terms. Philos. Trans. R. Soc. Lond. B Biol. Sci. 373, 20170136. https://doi.org/10.1098/rstb.2017.0136.

Rice, G.E., Hoffman, P., Lambon Ralph, M.A., 2015a. Graded specialization within and between the anterior temporal lobes. Ann. N. Y. Acad. Sci. 1359, 84–97. https://doi.org/10.1111/nyas.12951.

Rice, G.E., Lambon Ralph, M.A., Hoffman, P., 2015b. The roles of left versus right anterior temporal lobes in conceptual knowledge: an ALE meta-analysis of 97 functional neuroimaging studies. Cerebr. Cortex 25, 4374–4391. https://doi.org/10.1093/cercor/bhv024.

Rogers, T.T., Hocking, J., Noppeney, U., Mechelli, A., Gorno-Tempini, M.L., Patterson, K., Price, C.J., 2006. Anterior temporal cortex and semantic memory: reconciling findings from neuropsychology and functional imaging. Cognit. Affect Behav. Neurosci. 6, 201–213. https://doi.org/10.3758/CABN.6.3.201.

Seghier, M.L., 2012. The angular gyrus: multiple functions and multiple subdivisions. Neuroscience 19, 43–61. https://doi.org/10.1177/1073858412440596.

Shinn, A.K., Baker, J.T., Lewandowski, K.E., Öngür, D., Cohen, B.M., 2015. Aberrant cerebellar connectivity in motor and association networks in schizophrenia. Front. Hum. Neurosci. 9, 1–16. https://doi.org/10.3389/fnhum.2015.00134.

Smith, S.M., 2002. Fast robust automated brain extraction. Hum. Brain Mapp. 17, 143–155. https://doi.org/10.1002/hbm.10062.

Smith, S.M., Nichols, T.E., 2009. Threshold-free cluster enhancement: addressing problems of smoothing, threshold dependence and localisation in cluster inference. Neuroimage 44, 83–98. https://doi.org/10.1016/j.neuroimage.2008.03.061.

Snowden, J.S., Thompson, J.C., Neary, D., 2004. Knowledge of famous faces and names in semantic dementia. Brain 127, 860–872. https://doi.org/10.1093/brain/awh099.

Sormaz, M., Jefferies, E., Bernhardt, B.C., Karapanagiotidis, T., Mollo, G., Bernasconi, N., Bernasconi, A., Hartley, T., Smallwood, J., 2017. Knowing what from where: hippocampal connectivity with temporoparietal cortex at rest is linked to individual differences in semantic and topographic memory. Neuroimage 152, 400–410. https://doi.org/10.1016/j.neuroimage.2017.02.071.

Sormaz, M., Murphy, C., Wang, H., Hymers, M., Karapanagiotidis, T., Poerio, G., et al., 2018. Default mode network can support the level of detail in experience during active task states. Proc. Natl. Acad. Sci. 115 (37), 9318–9323. https://doi.org/10.1073/pnas.1721259115.

Teige, C., Mollo, G., Millman, R., Savill, N., Smallwood, J., Cornelissen, P.L., Jefferies, E., 2018. Dynamic semantic cognition: characterising coherent and controlled

conceptual retrieval through time using magnetoencephalography and chronometric transcranial magnetic stimulation. Cortex 103, 329–349. https://doi.org/10.1016/j.cortex.2018.03.024.

Thompson-Schill, S.L., D'Esposito, M., Aguirre, G.K., Farah, M.J., 1997. Role of left inferior prefrontal cortex in retrieval of semantic knowledge: a reevaluation. Proc. Natl. Acad. Sci. U. S. A. 94, 14792–14797. https://doi.org/10.1073/pnas.94.26.14792.

Thompson, S.A., Patterson, K., Hodges, J.R., 2003. Left/right asymmetry of atrophy in semantic dementia: behavioral-cognitive implications. Neurology 61, 1196–1203. https://doi.org/10.1212/01.WNL.0000091868.28557.B8.

Turnbull, A., Wang, H.-T., Schooler, J.W., Jefferies, E., Margulies, D.S., Smallwood, J., 2018. The ebb and flow of attention: between-subject variation in intrinsic connectivity and cognition associated with the dynamics of ongoing experience. Neuroimage 185, 286–299. https://doi.org/10.1016/j.neuroimage.2018.09.069.

van Heuven, W.J.B., Mandera, P., Keuleers, E., Brysbaert, M., 2014. SUBTLEX-UK: a new and improved word frequency database for British English. Q. J. Exp. Psychol. 67, 1176–1190. https://doi.org/10.1080/17470218.2013.850521.

Vatansever, D., Bzdok, D., Wang, H., Mollo, G., Sormaz, M., Murphy, C., Karapanagiotidis, T., Smallwood, J., Jefferies, E., 2017. Varieties of semantic cognition revealed through simultaneous decomposition of intrinsic brain connectivity and behaviour. Neuroimage 158, 1–11. https://doi.org/10.1016/j.neuroimage.2017.06.067.

Visser, M., Jefferies, E., Embleton, K.V., Lambon Ralph, M.a., 2012. Both the middle temporal gyrus and the ventral anterior temporal area are crucial for multimodal semantic processing: distortion-corrected fMRI evidence for a double gradient of information convergence in the temporal lobes. J. Cogn. Neurosci. 24, 1766–1778. https://doi.org/10.1162/jocn_a_00244.

Wagner, A.D., Paré-Blagoev, E.J., Clark, J., Poldrack, R.A., 2001. Recovering meaning. Neuron 31, 329–338. https://doi.org/10.1016/S0896-6273(01)00359-2.

Wang, D., Buckner, R.L., Liu, H., 2014. Functional specialization in the human brain estimated by intrinsic hemispheric interaction. J. Neurosci. 34, 12341–12352. https://doi.org/10.1523/JNEUROSCI.0787-14.2014.

Wang, H.T., Bzdok, D., Margulies, D., Craddock, C., Milham, M., Jefferies, E., Smallwood, J., 2018a. Patterns of thought: population variation in the associations between large-scale network organisation and self-reported experiences at rest. Neuroimage 176, 518–527. https://doi.org/10.1016/j.neuroimage.2018.04.064.

Wang, H.T., Poerio, G., Murphy, C., Bzdok, D., Jefferies, E., Smallwood, J., 2018b. Dimensions of experience: exploring the heterogeneity of the wandering mind. Psychol. Sci. 29, 56–71. https://doi.org/10.1177/0956797617728727.

Wang, X., Bernhardt, B.C., Karapanagiotidis, T., De Caso, I., Gonzalez Alam, T.R. del J., Cotter, Z., Smallwood, J., Jefferies, E., 2018. The structural basis of semantic control: evidence from individual differences in cortical thickness. Neuroimage 181, 480–489. https://doi.org/10.1016/j.neuroimage.2018.07.044.

Whitney, C., Kirk, M., O'Sullivan, J., Lambon Ralph, M.A., Jefferies, E., 2011. The neural organization of semantic control: TMS evidence for a distributed network in left inferior frontal and posterior middle temporal gyrus. Cerebr. Cortex 21, 1066–1075. https://doi.org/10.1093/cercor/bhq180.

Wilson, M., 1988. MRC psycholinguistic Database : machine-useable dictionary , version 2.00. Behav. Res. Methods Instrum. Comput. 20, 6–10.

Woolrich, M., 2008. Robust group analysis using outlier inference. Neuroimage 41, 286–301. https://doi.org/10.1016/j.neuroimage.2008.02.042.

Woolrich, M.W., Behrens, T.E.J., Beckmann, C.F., Jenkinson, M., Smith, S.M., 2004. Multilevel linear modelling for FMRI group analysis using Bayesian inference. Neuroimage 21, 1732–1747. https://doi.org/10.1016/j.neuroimage.2003.12.023.

Yarkoni, T., Poldrack, R.A., Nichols, T.E., Van Essen, D.C., Wager, T.D., 2011. Large-scale automated synthesis of human functional neuroimaging data. Nat. Methods 8, 665–670. https://doi.org/10.1038/nmeth.1635.

Yeo, B.T.T., Krienen, F.M., Sepulcre, J., Sabuncu, M.R., Lashkari, D., Hollinshead, M., Roffman, J.L., Smoller, J.W., Zollei, L., Polimeni, J.R., Fischl, B., Liu, H., Buckner, R.L., 2011. The organization of the human cerebral cortex estimated by intrinsic functional connectivity. J. Neurophysiol. 106, 1125–1165. https://doi.org/10.1152/jn.00338.2011.

Zhang, Y., Brady, M., Smith, S., 2001. Segmentation of brain MR images through a hidden Markov random field model and the expectation-maximization algorithm. IEEE Trans. Med. Imaging 20, 45–57. https://doi.org/10.1109/42.906424.